

HIGH RESOLUTION FABRY-PEROT AND MULTI-PUPIL SPECTRAL OBSERVATIONS OF THE GENUINE BLUE COMPACT DWARF GALAXY IZW18

A.R.PETROSIAN¹, G.COMTE², J.BOULESTEIX², D.KUNTH³,
T.MOVSESIAN¹, S.DODONOV⁴, E.LE COARER², A.BURENKOV⁴

1. Byurakan Astrophysical Observatory, Armenia
2. Marseille Observatory, France
3. Institut d'Astrophysique de Paris, France
4. Special Astrophysical Observatory, Russia

We present the observations of the BCDG IZW18 performed with a Fabry-Perot interferometer at the CFH 3.6m telescope and with a multi-pupil spectrograph at the SAO (Russia) 6m telescope. Morphological structure of the galaxy in emission lines and in continuum, the velocity field of the ionized gas and [OIII]/H α ratio distribution along the NW component have been investigated. Besides the NW and SE HII components, we find a population of small HII regions. Continuum maps show that the peaks of the stellar light distribution are displaced with respect to the emission lines maxima. The velocity field shows peculiar motions superposed on a approximately regular background implying solid body rotation. Emission line profiles exhibit asymmetric structure, except for the NW compact component [OIII]/H α ratio decreases from the centre of the NW component to its edge with the gradient of 1.86 kpc⁻¹.

1. *Introduction.* The dwarf galaxy IZW18 is a well known object belonging to the class of Blue Compact Dwarf Galaxies (BCDGs). After determination that this galaxy has lowest abundance for a Population I object in the Universe (Searle & Sargent 1972; Lequeux et al 1979; French 1980; Kinman & Davidson 1981) the interest on it rapidly has been increased. Last about 15 years more than 50 scientific papers have been addressed to IZw18. Among these articles which contain data on IZw18 as an extended, two component system (Petrosian et al 1978; Mazzarella & Boroson 1993) are very rare. A few imaging studies (e.g Davidson et al 1989; Dufour & Hester 1990) have shown that besides of two NW and SE components the galaxy has more complex structure. Because of its high surface brightness the NW component has been the target of more detail investigation. For it has been found: (i) the existence

of different spatial structure in stellar continuum and emission line lights (Davidson et al 1989); (ii) the lowest oxygen abundance (e.g. Skillman & Kennicutt 1993); (iii) the existence of the underlying, broad (about 3600 km s^{-1}) H_{α} emission (Skillman & Kennicutt 1993).

As part of the program of high spatial and spectral resolution study of genuine BCDGs, in this paper we present results of Fabry-Perot interferometric observations of IZW18 and multi-pupil spectroscopy of its NW component. We shall adopt 10 Mpc as the distance to IZW18, and a Hubble constant $H_0 = 75 \text{ km s}^{-1} \text{ Mpc}^{-1}$.

2. Observations and data reduction

2.1. Fabry-Perot interferometry. Observations have been performed at the Cassegrain focus of the 3.6m Canada-France-Hawaii telescope with the CIGALE instrument (see details in Boulesteix et al 1983).

CIGALE observations enable us to separate monochromatic emission from con-

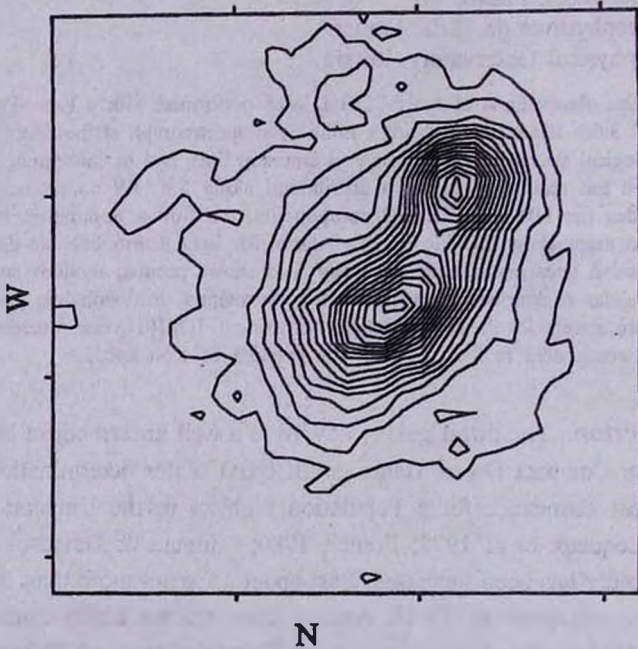


Fig. 1. Integrated 6600A red continuum intensity map of IZW18. The lowest contour corresponds to a flux of a $1.2 \cdot 10^{-18} \text{ ergs cm}^{-2} \text{ s}^{-1}$ per pixel. Contours are logarithmically spaced with levels separated by a factor 0.1. Condensations observed in red continuum are marked.

tinuum emission (Laval et al 1987). The continuum subtracted H_{α} line images of IZW18 were calibrated using the absolute flux published by Davidson & Kinman (1985) and Dufour & Hester (1990). In the same way a continuum map in the bandwidth of 10A free from H_{α} line contribution was built.

2.2. Multi-pupil spectroscopy. The observations have been performed at the Prime focus of the 6m telescope of SAO (Russia) with the multi-pupil spectrophotometer, provided bidimensional spectroscopy of the object. The array 9×11 square microlenses were used. The image scale constructed by one lens was $1.25'' \times 1.25''$. Two spectral regions have been observed: blue (4600-5200AA) and red (6200-6800AA) with dispersion of about 1A per pixel. 99 spectra were simultaneously registered on the two dimensional photon counting system.

3. Results. When the interferometer is scanning the object, the monochromatic emission of this latter is modulated by the interference pattern while the continuum emission remains unaffected. This enables to distinguish line and continuum emission with a much higher contrast than with simple images obtained through interference filters. Figures 1 and 2 show the contour maps of respectively the continuum emission

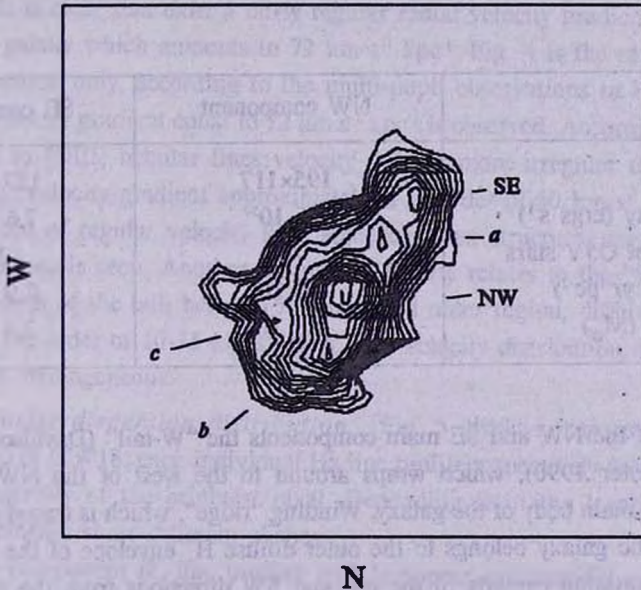


Fig. 2. Integrated H_{α} line intensity map of IZW18. The lowest contour corresponds to a flux of a $1.0 \cdot 10^{-17}$ ergs $\text{cm}^{-2} \text{s}^{-1}$ per pixel. Contours are spaced with levels separated by a factor 1.58.

and the monochromatic H_{α} emission in absolute flux units across the main body of IZW18 (1.'5×1.'4 field).

3.1 Red continuum morphology. In continuum light besides of two NW and SE components (Davidson et al 1989) a third one (a) is observed half way between them. We identify two other condensations: (b) to the north and (d) to the N-W of the NW compact component. Continuum radiation of IZW18 extends in the NE and SW directions to distances at least 740 pc from the brightest NW component.

3.2. H_{α} morphology. Our H_{α} image completely reproduces the structural features which were identified in early H_{α} observations of IZW18 (Hua et al 1987; Davidson et al 1989; Dufour & Hester 1990).

Both NW and SE condensations are isolated from the main body of the galaxy by an isophote corresponding to $4.5 \cdot 10^{-15}$ ergs $\text{cm}^{-2} \text{s}^{-1} \text{arcsec}^{-2}$ of surface brightness. In Table 1 for NW and SE components for this level of surface brightness are presented: linear size; correcting for Galactic reddening the integrated H_{α} luminosity; assuming Case B conditions, $T_e = 18000$ K (Dufour et al 1988) and according to Osterbrock (1989) the number of O5V stars; assuming a Salpeter initial mass function, star formation rates of all stars (0.1 to $100M_{\odot}$); the mass of the ionized gas.

Table 1

	NW component	SE component
Size (pc^2)	195×117	157×117
Luminosity (ergs s^{-1})	$1.6 \cdot 10^{39}$	$7.6 \cdot 10^{38}$
Number of O5V stars	47	23
SFR ($M_{\odot} \text{yr}^{-1} \text{pc}^{-2}$)	$4.7 \cdot 10^{-7}$	$2.9 \cdot 10^{-7}$
HII mass (M_{\odot})	$7.3 \cdot 10^5$	$3.4 \cdot 10^5$

Besides of the NW and SE main components the "W-tail" (Davidson et al 1989; Dufour & Hester 1990), which wraps around to the west of the NW component, belongs to the main body of the galaxy. Winding "ridge", which is traced only by outer isophotes of the galaxy belongs to the outer diffuse H_{α} envelope of the main body.

The H_{α} emission extends in the NE and SW directions from the main body of IZW18, to distances at least 1.2 kpc. The extended envelope detected in H_{α} line is not simply diffuse, it shows numerous condensations. These condensations are thought to be HII regions. A total of 39 HII regions, from which only three show counterparts in

red continuum, were identified. They have been detected on the total H_{α} map and their presence on at least two consecutive channel maps has been checked. The limits of each region are defined at the contour where the intensity of the H_{α} emission falls to the average local intensity of the diffuse component.

3.3 HII regions size distribution and luminosity function. The size distribution of HII regions is consistent with an exponential $N = N_0 \exp(D/D_0)$ with $D_0 = 24 \text{ pc}$. This can be compared to the characteristic D_0 values found for Magellanic Irregular galaxies (Hodge et al 1989; Hodge & Lee 1990).

For IZW18 the small number of HII regions prevents a derivation of an accurate luminosity function, but nevertheless the data are sufficient to get a first approximation. The observed luminosity function of IZW18 shows a turnover with maximum at $L = 3.0 \cdot 10^{36} \text{ ergs s}^{-1}$. This turnover is due to incompleteness of the sample towards fainter luminosities. At luminosities brighter than this turnoff the observed function is reasonably well fitted by a power law $N(L) = AL^{\alpha} dL$ of slope $\alpha = -1.6 \pm 0.3$. This is consistent with the mean value derived for dwarf irregular galaxies (Strobel et al 1991) $\alpha = -1.5 \pm 0.3$.

3.4. H_{α} velocity field. Fig. 3 is the velocity field superposed on the H_{α} map of the galaxy. It is clear that exist a fairly regular radial velocity gradient over of main body of the galaxy which amounts to $73 \text{ km s}^{-1} \text{ kpc}^{-1}$. Fig. 4 is the same cut, on the NW condensation only, according to the multi-pupil observations in H_{β} line. In this case radial velocity gradient equal to $72 \text{ km s}^{-1} \text{ kpc}^{-1}$ is observed. According to the same observations in [OIII] nebular lines velocity field is more irregular than in Balmer lines, existed velocity gradient approximately is in order of $60 \text{ km s}^{-1} \text{ kpc}^{-1}$. Against the background of regular velocity field some complex structure, suggesting lots of turbulent motions is seen. Another interesting feature relates to the "W-tail". Along the whole length of the tail, between its inner and outer region, differences in radial velocities of the order of $10\text{-}15 \text{ km s}^{-1}$ exist, The velocity distribution in the southern ridge is more homogeneous.

3.5. Velocity dispersion distribution. Fig. 5 displays, superposed to the H_{α} isophotal map of IZW18, each individual H_{α} line profile respectively normalized to the maximum intensity of the brightest pixel. Depending from the location across the galaxy line profiles show different shapes.

The NW component H_{α} line profiles mainly appear symmetrical and well represented by a one component Gaussian fit. The same is correct for H_{β} and [OIII] lines. Averaged over NW component and corrected for the instrumental profile FWHMs of Balmer as well forbidden lines are in the order of 90 km s^{-1} . Because of small free spectral range (375 km s^{-1}) for Fabry-Perot observations and low signal to noise ratio

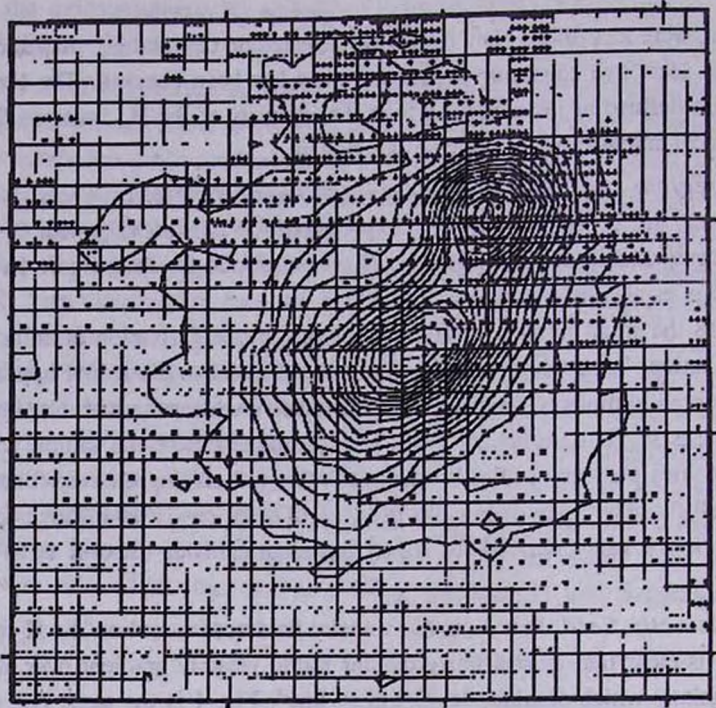


Fig. 3. Velocity field of IZW18 superposed on the H_{α} map of the galaxy.

($S/N=10$ near H_{α}) for multi-pupil observations we have no chance to detect broad (FWHM about 3600 km s^{-1}) component of H_{α} line (Skillman & Kennicutt 1993).

All H_{α} line profiles observed in pixels belonging to the SE component are asymmetric with blue side excesses. Blue component in average is shifted in order of 50 km s^{-1} .

A striking difference is seen between line profiles of the regions corresponding to the "W-tail" and southern ridge of the galaxy. Across the southern ridge, as a whole, profiles with strong blue side asymmetry are typical (two components with about 40 and 80 km s^{-1} shift). In the western tail all regions show red (in order to 50 km s^{-1}) as well blue (in order to 40 km s^{-1}) shifted excesses of velocities. In the outer envelope of the main body, profiles also are asymmetric with red wings in N-NW and the west of the SE component, and blue wings elsewhere.

3.6. $[OIII]/H_{\beta}$ ratio distribution along of NW component. Fig. 6 is a position- $[OIII]/H_{\beta}$ ratio cut across the optical major axis of the galaxy ($PA=143^{\circ}$). Pre-

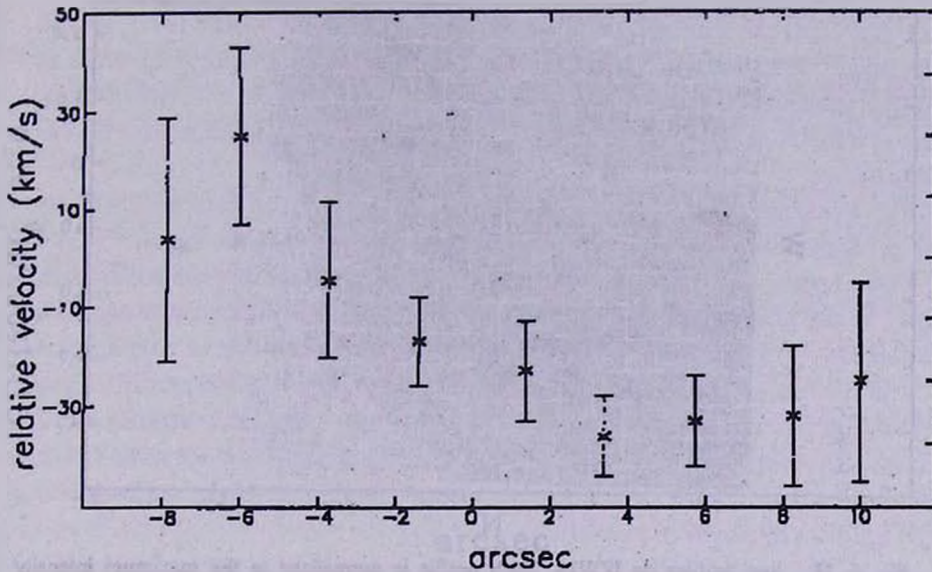


Fig. 4. Position velocity cut across the optical major axis of the galaxy (PA= 143°) in $H\beta$ line. Data are averaged within the 30° sector around the PA.

sented data are averaged within the 30° sector around the PA. It is clear from the Fig. 6 that there is a fairly regular, with gradient of $0.0893 \text{ arcsec}^{-1}$, decreasing of the $[\text{OIII}]/H\beta$ ratio from the center of the component to its edge.

According to Skillman & Kennicutt (1993) there is tentative indication of a radial gradient in electron temperature ($0.13 \cdot 10^4 \text{ K arcsec}^{-1}$) and no any in electron density for the NW component. We can conclude that ionic abundance of O^{++} which strongly depends from $[\text{OIII}]/H\beta$ ratio and electron temperature as well electron density increase from the centre to the edge of the NW component with the gradient equal to $9.25 \cdot 10^{-7} \text{ arcsec}^{-1}$. The gradient mainly attributable to the difference in the measured electron temperatures. Unfortunately we have no any information regarding to the distribution of $3727[\text{OII}]/H\beta$ ratio across to the NW component. So it is difficult to do conclusion about oxygen abundance distribution across the component.

4. Discussion.

4.1. *The structure.* Is IZW18 an old system in which some intense episodes of star formation already occurred, or does it form stars for the first time? Loose & Thuan

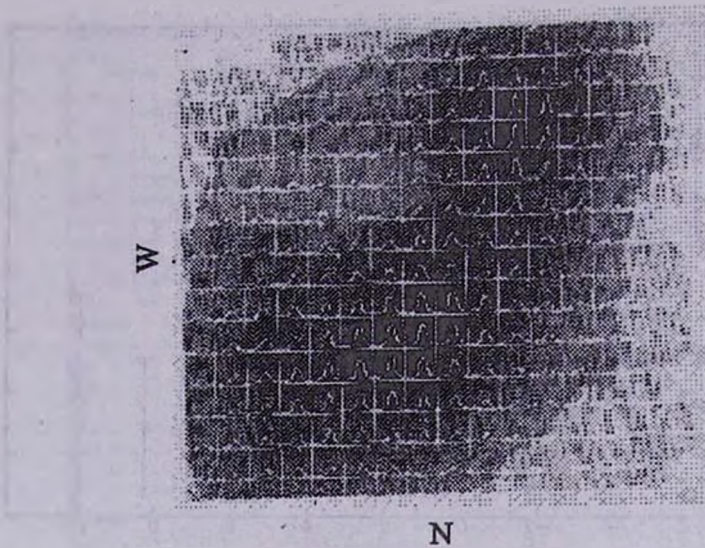


Fig. 5. H_{α} line profiles on IZW18. Each profile is normalized to the maximum intensity of the brightest pixel.

(1986) reported observations of a faint outer component of extended stellar continuum which they attributed to an underlying old population. Thuan (1983) from detected infrared emission, Hua et al (1987), Davidson et al (1989), Dufour & Hester (1990) from red continuum imagery, confirmed the presence of this component.

We have shown that in red continuum light at least three additional brightness concentrations are seen besides the already known compact NW and SE sources. The NW and SE components have an H_{α} peak brightness displaced from the red continuum peak position.

In the following, we make the assumption that H_{α} peaks are related to the current star forming regions and red continuum peaks to the recent or past sites of star formation. The distribution of star forming regions in IZW18 shows a chain like structure. Out of seven identified current and past star forming knots 6 are distributed along a line. The chain of star forming knots is positioned in the direction of elongation of the main body of IZW18 and its position is quite consistent with HI clumps distribution in the vicinity of the galaxy (Lequeux & Viallefond 1980).

In the chain both NW and SE current star forming regions are located between recent or old star forming sites. Is this geometry a random configuration? Does it exemplify the sequential nature of star formation events in the galaxy (Kunth et al. 1988)? Stochastic self propagating star formation simulations of star formation sites

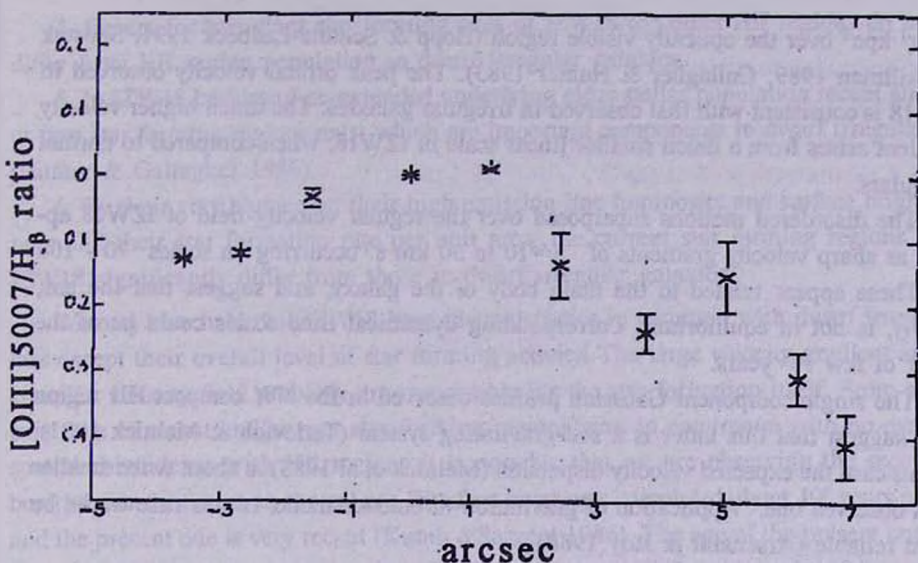


Fig. 6. Position-[OIII]/H_β ratio cut across the optical major axis of the galaxy (PA= 143°). Data are averaged within the 30° sector around the PA.

in dwarf galaxies show that the properties of dwarf systems predicted by these models depend on the size ratio of the galaxy to the star formation cells. Small galaxies similar to IZW18 which evolve mainly via a series of disconnected star forming bursts (e.g. Hunter & Gallagher 1986). Therefore, a random origin of the observed "chain" is more plausible. The only evidence is that the main body of IZW18 consists of two separated star forming areas with associated current and recent or old star forming regions which is confirmed by the differences in velocity between the two main compact components (744 ± 10 km s⁻¹ and 782 ± 6 km s⁻¹ respectively for NW and SE components).

4.2. The kinematics and dynamics. What is the mechanism which triggers the subsequent star formation in IZW18? The velocity field may play an important role. The ordered component of the velocity field shows a peak orbital velocity of 45 km s⁻¹. The velocity gradient observed across the offsetted HI peak distribution is 50 km s⁻¹ kpc⁻¹ (Viallefond et al 1987) compared to the about 70 km s⁻¹ kpc⁻¹ observed along the main star forming regions, both in H_α (our results in Sec. 3.4) and in HI (from the maps of Viallefond et al 1987).

Most irregular galaxies (giant as well as dwarf), exhibit a solid body rotation with peak orbital velocities of 50-70 km s⁻¹ but shallow velocity gradients of 5-20

$\text{km s}^{-1} \text{ kpc}^{-1}$ over the optically visible region (Hopp & Schulte-Ladbeck 1991; Shostak & Skillman 1989; Gallagher & Hunter 1983). The peak orbital velocity observed in IZW18 is consistent with that observed in irregular galaxies. The much higher velocity gradient arises from a much smaller linear scale in IZW18, when compared to normal irregulars.

The disordered motions superposed over the regular velocity field of IZW18 appear as sharp velocity gradients of $V=10$ to 30 km s^{-1} occurring on scales $70 - 100 \text{ pc}$. These appear related to the main body of the galaxy, and suggest that the gas, locally, is not in equilibrium. Corresponding dynamical time scales could be of the order of few 10^6 years.

The single component Gaussian profiles observed in the NW compact HII region may suggest that this latter is a self-gravitating system (Terlevich & Melnick 1981). In this case the expected velocity dispersion (Melnick et al 1988) is about twice smaller than observed one. Application of gravitation-turbulence model in this case would be more reliable (Arsenault & Roy 1988).

In the SE compact HII region the velocity dispersion for the main Gaussian component (about 19 km s^{-1}) is higher than it is expected from self-gravitational model (Terlevich & Melnik 1981). The excess velocity dispersion can be caused by the gravity of (a) and SE recent or old star forming regions. The fitted much weaker second Gaussian component can be another isolated HII region in SE area, not distinguishable because of projection effects.

The complex structure of the H_α line profiles observed in the envelope around the main body of the galaxy, with variable asymmetry suggests that we observe gas infall onto the main body of the galaxy, whatever the direction of observation.

4.3. *The nature of IZW18.* We examine the nature of IZW18 following the hypothesis that in general BCDGs may be considered as the low luminosity end of irregular galaxies (Searle & Sargent 1972, Vigroux et al 1986, Kunth et al 1986, Thuan 1987). The results of comparison of the properties of IZW18 with that of dwarf irregular galaxies may be summarized as follows.

1. IZW18 has an absolute luminosity consistent with that of an "average" dwarf irregular. The small linear size of IZW18 gives a high surface brightness of the optically visible component.

2. HI masses of IZW18 and dwarf irregular galaxies of comparable blue luminosity and the clumpy structure of the HI distribution are similar.

3. A rigid body rotation similar to that observed in dwarf irregular galaxies with quite similar peak orbital velocity is observed in IZW18. The size of IZW18 makes the velocity gradient across it at least 5 times higher than in irregular galaxies.

4. Except for two giant star forming sites of IZW18 the other HII regions do not differ from HII region population in dwarf irregular galaxies.

5. In IZW18 besides of an extended underlying older stellar population recent and/or past star forming regions exist which are important components in dwarf irregulars (Hunter & Gallagher 1986).

6. By their very blue color, their high emission line luminosity and surface brightness and their star formation rate per unit area, the current star forming regions in IZW18 significantly differ from those in dwarf irregular galaxies.

We may conclude that IZW18 have characteristics in common with dwarf irregulars except their overall level of star forming activity. The large velocity gradient and complex velocity field probably are responsible for the star formation itself. From the existence of recent and/or past star forming regions seen in continuum with no exact spatial coincidence with HII regions it is possible that we are observing the second burst of star formation in the galaxy. The first burst was completed about 10^9 years ago and the present one is very recent (Kunth & Sargent 1986). The age of the present burst may be estimated as a few 10^6 years (Lequeux et al 1981; Copetti et al 1984).

ФАБРИ-ПЕРО И МНОГОЗРАЧКОВЫЕ СПЕКТРАЛЬНЫЕ НАБЛЮДЕНИЯ ВЫСОКОГО РАЗРЕШЕНИЯ ИСТИННОЙ ГОЛУБОЙ КОМПАКТНОЙ КАРЛИКОВОЙ ГАЛАКТИКИ IZW18

А.Р.ПЕТРОСЯН, Г.КОНТ, Дж.БУЛЕСТЕКС, Д.КУНТ,
Т.МОВСЕСЯН, С.ДОДОНОВ, Е.ЛЕ КОАРЕР, А.БУРЕНКОВ

Представлены результаты наблюдений Голубой Компактной Карликовой Галактики IZW18, выполненных с Фабри-Перо интерферометром на Канадо-Франко-Гавайском 3.6м телескопе и с многозрачковым спектрографом на 6м телескопе САО (Россия). Были исследованы морфологическая структура галактики в эмиссионных линиях и в континууме, поле скоростей эмиссионного газа и распределение отношения $[OIII]/H_{\beta}$ вдоль северо-западного (NW) компонента. Кроме северо-западного (NW) и юго-восточного (SE) компонентов отождествлено семейство маленьких HII областей. Показано, что максимумы звездного компонента галактики смещены по сравнению с таковыми для газового

компонента. Поле скоростей показывает пекулярные движения на фоне приблизительно регулярного движения. Профили эмиссионных линий NW компонента симметричны, остальные в основном асимметричны. Отношение $[OIII]/H\beta$, с градиентом 1.86 Кпк-1, уменьшается от центра NW компонента к его краю. Обнаружено; что "сгусток" Цвикки - это маленькая III область с одинаковой как у IZW18 радиальной скоростью.

REFERENCES

- R.Arsenault, J.-R.Roy*, 1988, *A&A*, 201, 199.
J.Boulesteix, Y.P.Georgelin, M.Marcelin, G.Monnet, 1983, *SPIE Conf. Instr. Astron.*, 445, 37 *opetti M. V. F., Pastoriza M. G., Dottori H.A.*, 1985, *A&A*, 152, 427.
K.Davidson, T.D.Kinman, 1985, *ApJ*, 58, 321.
K.Davidson, T.D.Kinman, S.D.Friedman, 1989, *AJ*, 97, 1591.
R.J.Dufour, 1986, *PASP*, 98, 1025.
R.J.Dufour, J.J.Hester, 1990, *ApJ*, 350, 149.
J.S.Gallagher, D.A.Hunter, 1983, *ApJ*, 274, 141.
H.B.French, 1980, *ApJ*, 240, 41.
P.W.Hodge, M.G.Lee, Jr.R.C.Kennicutt, 1989, *PASP*, 101, 32.
P.W.Hodge, M.G.Lee, 1990, *PASP*, 102, 26.
U.Hopp, R.E.Schulte-Ladbeck, 1991, *A&A*, 248, 1.
C.T.Hua, B.Grundseth, T.Nguyen-Trong, 1987, *Ap. Letters Comm.*, 25, 187.
D.A.Hunter, J.S.Gallagher, 1986, *PASP*, 98, 5.
Jr.R.C.Kennicutt, B.K.Edgar, P.W.Hodge, 1989, *ApJ*, 337, 761.
D.Kunth, W.L.W.Sargent, 1986, *ApJ*, 300, 496.
D.Kunth, S.Maurogordato, L.Vigroux, 1988, *A&A*, 204, 10.
D.Kunth, F.Sevre, 1986, *Star Forming Dwarf Galaxies*, (eds. D.Kunth, T.X.Thuan, J.T.T.Van), Editions Frontieres, p. 331.
A.Laval, J.Boulesteix, Y.P.Georgelin, Y.M.Georgelin, M.Marselin, 1987, *A&A*, 175, 199.
J.Lequeux, F.Viallefond, 1980, *A&A*, 91, 269.

- J.Lequeux, M.Peimbert, J.F.Rayo, A.Serrano, S.Torres-Peimbert*, 1979, *A&A*, 80, 155.
- J.Lequeux, M.Maucherat-Joubert, J.M.Deharveng, D.Kunth*, 1981, *A&A*, 103, 305.
- H.-H.Loose, T.X.Thuan*, 1986, *Star Forming Dwarf Galaxies*, (eds. D.Kunth, T.X.Thuan, J.T.T.Van), Editions Frontieres, p. 73.
- J.M.Mazzarella, T.A.Boroson*, 1993, *ApJS*, 85, 27.
- J.Melnick, R.Terlevich, M.Moles*, 1988, *MN*, 235, 297.
- D.E.Osterbrock*, 1989, *Astrophysics of Gaseous Nebulae and Active Galactic Nuclei* (University Science Books: Mill Valley, CA).
- A.R.Petrosian, K.A.Saakian, E.E.Khachikian*, 1978, *Astrophysics*, 14, 36.
- L.Searle, W.L.W.Sargent*, 1972, *AJ*, 173, 25.
- G.S.Shostak, E.D.Skillman, E.Brinks*, 1991, *BAAS*, 23, 920.
- E.D.Skillman, Jr.R.Kennicutt*, 1993, *ApJ*, 411, 655.
- N.V.Strobel, P.Hodge, Jr.R.C.Kennicutt*, 1991, *ApJ*, 383, 148.
- R.Terlevich, J.Melnick*, 1981, *MN*, 195, 839.
- T.X.Thuan*, 1983, *ApJ*, 268, 667.
- T.X.Thuan, T.B.Williams, E.Malumuth*, 1987, *Star Bursts and Galaxy Evolution* (eds. T.Montmerle, T.X.Thuan, T.T.Van), Editions Frontieres, p. 151.
- T.X.Thuan*, 1987, *Star Bursts and Galaxy Evolution*, (eds. T.Montmerle, T.X.Thuan, T.T.Van), Editions Frontieres, p. 129.
- F.Viallefond, J.Lequeux, G.Comte*, 1987, *Star Bursts and Galaxy Evolution*, (eds. T. Montmerle, T.X. Thuan, T.-T.Van), Editions Frontieres, p.139.
- F.Viallefond, T.X.Thuan*, 1983, *ApJ*, 269, 444.
- F.Zwicky*, 1966, *ApJ*, 143, 166.